Subcellular spatial proteomics by microscopy-guided photo-biotinylation reveals novel protein constituents in primary cilia

Yi-De Chen*, Chih-Wei Chang*, Chantal Hoi Yin Cheung*, Hsiao-Jen Chang*, Ya-Tien Fang, Yong-Da Sie, Chia-Wen Chung, Chun-Kai Huang, Weng Man Chong, Jung-Chi Liao#

Syncell Inc., Taipei, TAIWAN, * Co-authors, # Corresponding author (Email: jcliao@syncell.com)

De novo spatial proteomics

Abstract

Image-guided protein extraction at organelle-scale resolution holds significant promise for discovering novel protein constituents within disease- or function-related subcellular regions like primary cilia. Our firmware-integrated microscopy platform facilitates spatial protein purification through in situ subcellular photo-biotinylation at user-defined regions of interest (ROIs) one field of view (FOV) at a time, automatically processing thousands of FOVs. Illumination patterns of the ROI for each FOV are calculated in real-time using machine learning or traditional image processing. Light activation of amino acid crosslinkers is achieved by a two-photon laser in the platform, rendering precise protein biotinylation with 240-nanometer precision. A high-speed mechatronic control is implemented to coordinate imaging, pattern generation, targeted illumination, and FOV movement, allowing for the rapid biotinylation of millions of ROI spots within hours in cell or tissue samples. Once enough proteins are biotinylated, subsequent cell lysis, avidin pulldown and LC-MS/MS analysis unveil the subcellular proteome with exceptional sensitivity, specificity, and resolution. Using this technology, termed optoproteomics, we investigated the proteome of primary cilia in RPE-1 cells, identifying the proteome including 524 known ciliary proteins notably enriched. The top identified proteins encompassed key ciliary trafficking components and those involved in structural support and cellular organization. Gene ontology (GO) enrichment analysis highlighted the significant association of high-ranking proteins with critical ciliary processes such as assembly, transportation, and signaling, particularly includingproteins involved in intraciliary transport. A group of novel protein constituents were identified, providing testable hypotheses for their roles in primary cilia. These findings underscore the efficacy of targeted photolabeling and proteomic analysis in unraveling the network of proteins essential for ciliary function and structure, showcasing optoproteomics' potential for comprehensive subcellular spatial proteome discovery and its broad utility in cell biology for discovering novel protein compositions or biomarkers.

MICROSCOOP : hypothesis-free subcellular protein discovery platform

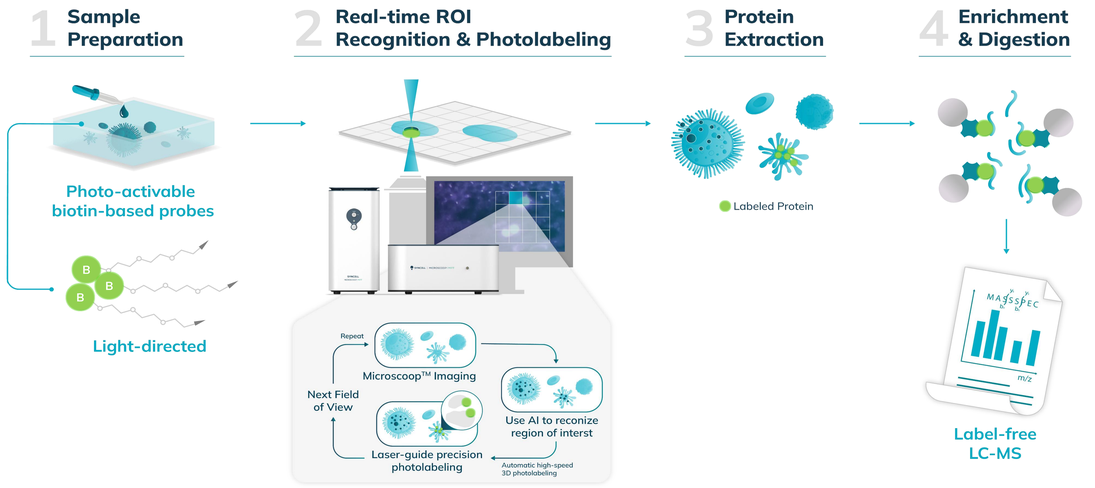

Fig. 1 | Schematic workflow of SYNCELL Microscoop™. A total-sync ultra-content microscopic platform that integrates image acquisition, photochemistry, microscopy, optics, and mechatronics enable high-content *in situ* photolabeling followed by mass spectrometry analysis.

MICROSCOOP : synchronized high-content system control at nanoscale resolution

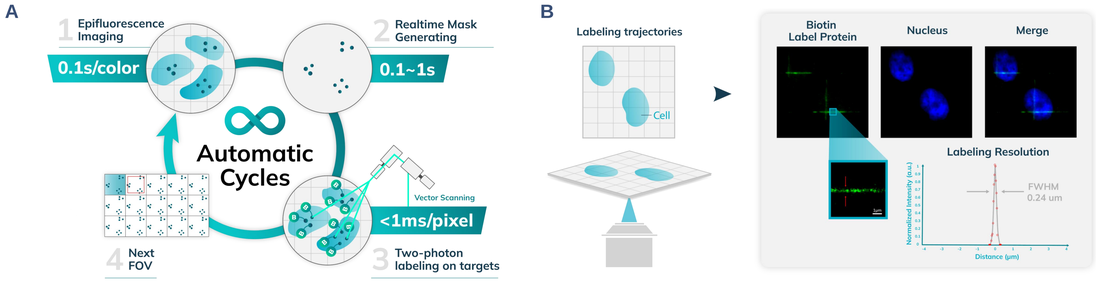

Fig. 2 | A, Workflow for ultrahigh-content targeted pohoto-biotinylation includes: (1) identifying and acquiring images of regions of interest by light microscope; (2) generating realtime patterns of ROIs; (3) illuminating the selected region within ROIs for protein photo-biotinylation; (4) moving the stage to the next FOV; and repeating steps 1-4 for each FOV until all FOVs have been processed. **B,** Resolution of photo-biotinylation. A line "cross" pattern is photolabeled on fixed U-2OS cells, and the biotinylated molecules are shown in green. DAPI: Blue, scale bar: 10 μm. 40x/0.95 NA objective.

MICROSCOOP : photo-induced biotinylation within primary cilia

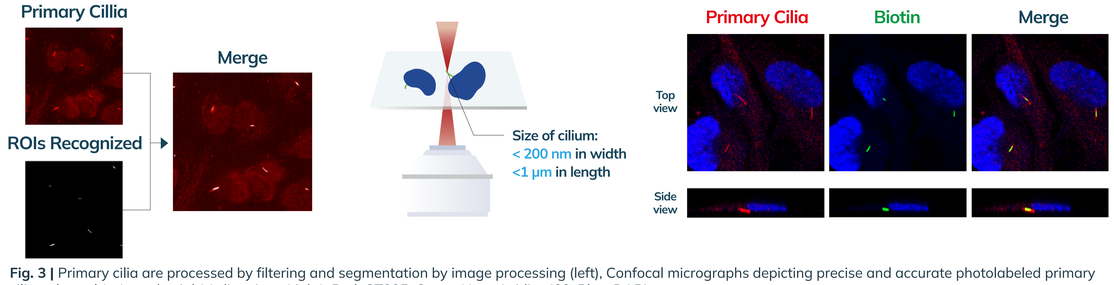

Fig. 3 | Primary cilia are processed by filtering and segmentation by image processing (left), Confocal micrographs depicting precise and accurate photolabeled primary cilia at lateral (xy)- and axial (z) directions (right). Red: GT335, Green: NeutrAvidin-488, Blue: DAPI.

MICROSCOOP : unveiling spatial proteomics of primary cilia and their functional insights

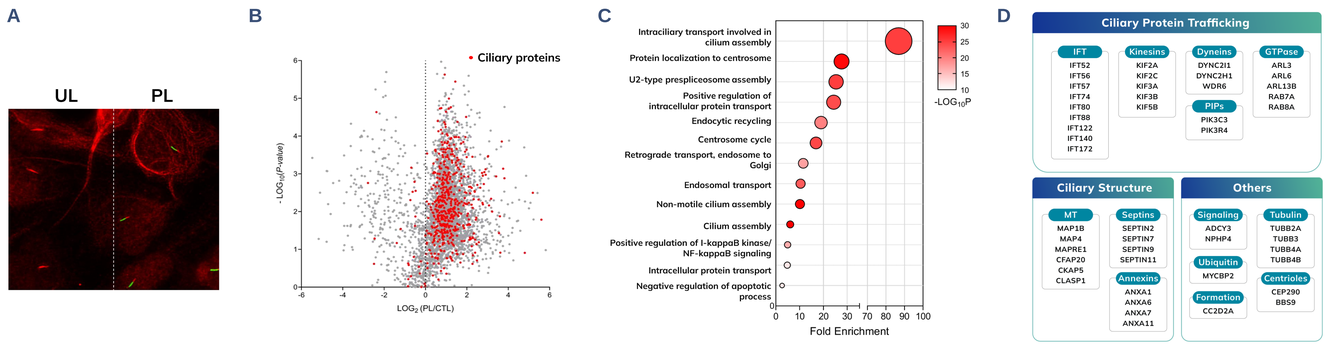

E

427 Ciliary proteins

ABCC4	ATG5	CCT5	CLUAP1	DNMT1	EXOC6	HSPA8	KIF2A	MYOF	PDXDC1	RAB10	SHROOM3	TNS3	VCP
ABLIM1	ATG7	CCT8	CNOT10	DPYSL2	EZR	HSPBP1	KIF3A	NCAPD2	PEX6	RAB1B	SLAIN2	TOGARAM2	VDAC3
ABRAXAS2	ATP1A1	CDK5RAP2	CNTRL	DROSHA	FKBP5	HSPD1	KIF3B	NCAPG	PFN2	RAB23	SLIRP	TP53BP1	VPS13A
ACLY	ATP1B1	CEP120	COL18A1	DSG2	FLNA	HUWE1	KIF5B	NDC80	PIBF1	RAB34	SLK	TPM3	VPS35
ACOT9	ATP2A2	CEP128	COPG1	DSTN	FNBP1L	HYDIN	KIF5C	NEK1	PIGS	RABEP2	SMARCA4	TRAPPC10	VTN
ACTN1	ATP2B4	CEP131	COPS8	DYNC1H1	FOCAD	HYOU1	KIFAP3	NEK6	PIK3C3	RAC1	SMPD4	TRAPPC3	VWA5A
ACTN4	ATP6V1A	CEP135	CROCC	DYNC1I2	GAK	IFIT3	KIFC1	NEK9	PIN1	RAN	SORD	TRAPPC9	WDHD1
ACTR1A	ATP6V1D	CEP152	CSNK1A1	DYNC2H1	GANAB	IFT122	KIRREL1	NIN	PJA2	RANGAP1	SPTAN1	TRIM59	WDR11
ACTR2	ATXN10	CEP164	CSNK2B	DYNC2I1	GLE1	IFT140	LDHB	NME7	POLA2	RHOT1	SQSTM1	TRIP11	WDR18
ACTR3	AURKA	CEP170	CTNNA1	EEF1A1	GLOD4	IFT172	LRBA	NOL6	POLD1	RPA1	SRR	TSC2	WDR19
ADD3	AXL	CEP192	CTNNB1	EFCAB7	GLRX3	IFT27	MACF1	NPHP4	POR	RPGRIP1L	SSX2IP	TSG101	WDR35
AKAP9	BBS1	CEP250	CTTN	EFTUD2	GMDS	IFT52	MAP1A	NUDC	PPA1	RPS6KA1	STAT3	TTC21B	WDR47
AKT1	BBS2	CEP290	CUL3	EGFR	GNA11	IFT56	MAP1B	NUP210	PPID	RPTOR	STIP1	TUBA1B	WDR5
ANKMY2	BBS4	CEP350	CYFIP2	EHD3	GOT2	IFT57	MAP1S	NUP214	PPP1CC	RRM1	STK33	TUBA4A	WDR62
ANXA11	BRI3BP	CEP43	CYLD	EIF2A	GRK2	IFT70A	MAP4	NUP35	PPP2R1A	RTCA	SUPT5H	TUBA4B	WIZ
ANXA6	C2CD3	CEP57	DCTN1	EIF2S1	GSK3B	IFT74	MAP4K3	NUP62	PRDX4	RUVBL1	SYNE1	TUBB2A	WRAP73
AP2A1	CALR	CEP63	DCTN2	EIF3A	GSN	IFT80	MAPKAP1	NUP93	PRIM1	RUVBL2	SYNE2	TUBB4B	YTHDF3
AP3M2	CALU	CEP76	DCTN3	EIF4B	HAT1	IFT88	MAPKBP1	OCRL	PRKAA1	SCCPDH	TAGLN2	TUBB6	YWHAE
APEX1	CAMK2D	CEP78	DCTN4	EIF4H	HAUS1	INPPL1	MAPRE1	ODF2	PRKAR2A	SCD	TAPT1	TUBGCP2	YWHAG
APP	CAMSAP1	CEP89	DDX1	EIF5A	HAUS3	INTS1	MDM1	OFD1	PRKAR2B	SCD5	TARS1	TUBGCP3	YWHAQ
APPL1	CAPN2	CEP97	DDX21	EIPR1	HAUS4	INTS2	MED16	OGFR	PRKCA	SDCCAG8	TBC1D31	TUBGCP4	ZC2HC1A
ARF4	CAPZB	CFAP20	DDX56	ELMO2	HAUS5	IPO5	MICAL3	ORC1	PRKD2	SEC23A	TCHP	TUBGCP6	ZFYVE26
ARHGAP1	CARS1	CHD4	DHX30	ELP4	HAUS6	IQCE	MLEC	P4HA1	PSMC2	SEPTIN10	TCP1	TXNL1	ZSCAN18
ARHGAP35	CASK	CHORDC1	DHX9	EML1	HDAC1	ITGA3	MROH2B	PACS1	PSMC5	SEPTIN11	THBS1	UBA1	ZWILCH
ARHGEF18	CAV1	CIT	DLG5	EPB41L3	HHIP	KATNAL1	MSN	PAFAH1B1	PSMD14	SEPTIN2	THOP1	UBA6	
ARL3	CC2D2A	CKAP2	DMD	EPS15	HK1	KATNAL2	MTCL1	PAPSS1	PSMD5	SEPTIN6	TIGAR	UBAP2L	
ARMC9	CCDC61	CKAP5	DNAAF5	EPS8L2	HMGB2	KATNB1	MXRA8	PCM1	PTPN23	SEPTIN7	TJP2	UBE3C	
ASAP1	CCDC88A	CLASP1	DNAH11	ERC1	HNRNPLL	KDM3B	MYADM	PCNT	PTPRK	SEPTIN9	TMEM231	UGGT1	
ASNS	CCP110	CLIC1	DNAJA1	EXOC3	HSP90AB1	KHSRP	MYH10	PDCD6IP	PUM1	SF3A1	TMPO	USP9X	
ATG16L1	CCT2	CLTB	DNAJB1	EXOC4	HSP90B1	KIF1B	MYO1E	PDE1C	PXDN	SF3B2	TMPO	VCAN	
ATG3	CCT4	CLTC	DNM2	EXOC5	HSPA4	KIF20A	MYO5A	PDGFRA	QKI	SH3GL1	TNPO1	VCL	

F

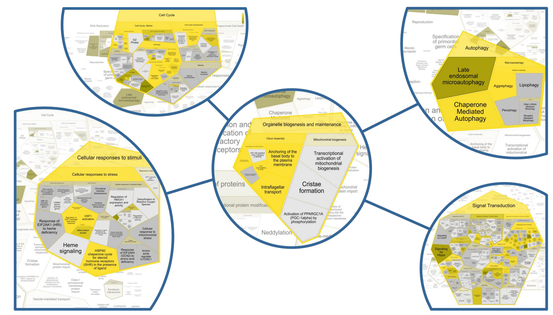

G

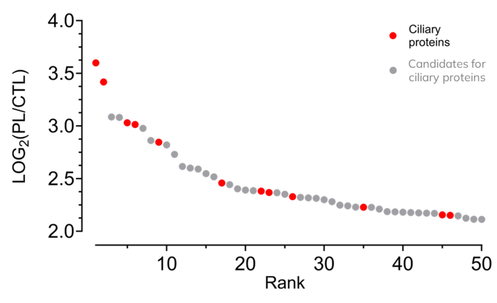

H

Gene name	Protein description
PPIB	Peptidyl-prolyl cis-trans isomerase B
ALDH1A3	Retinaldehyde dehydrogenase 3
CAVIN1	Caveolae-associated protein 1
SF3A3	Splicing factor 3A subunit 3
TRIM25	E3 ubiquitin/ISG15 ligase TRIM25
AP2A2	AP-2 complex subunit alpha-2
SRP72	Signal recognition particle subunit SRP72
CTNND1	Catenin delta-1
MARS1	Methionine--tRNA ligase, cytoplasmic
HNRNPDL	Heterogeneous nuclear ribonucleoprotein D-like
PNPLA6	Patatin-like phospholipase domain-containing protein 6
CPNE3	Copine-3
EPHA2	Ephrin type-A receptor 2
SUPT16H	FACT complex subunit SPT16
RPS7	Small ribosomal subunit protein eS7

Gene name	Protein description
CD2AP	CD2-associated protein
NUP98	Nuclear pore complex protein Nup98-Nup96
AP3B1	AP-3 complex subunit beta-1
GOLGA4	Golgin subfamily A member 4
CNOT1	CCR4-NOT transcription complex subunit 1
COPB1	Coatomer subunit beta
NPM1	Nucleophosmin
SERPINH1	Serpin H1
UACA	Uveal autoantigen with coiled-coil domains and ankyrin repeats
TKT	Transketolase
AARS1	Alanine--tRNA ligase, cytoplasmic
FLOT2	Flotillin-2
TJP1	Tight junction protein ZO-1
NXF1	Nuclear RNA export factor 1
ARPC1B	Actin-related protein 2/3 complex subunit 1B

I

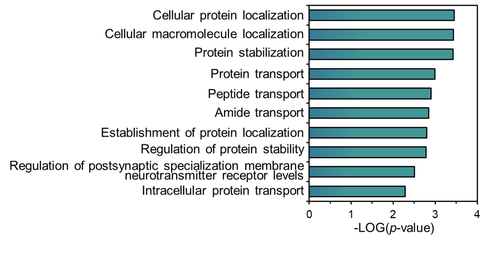

J

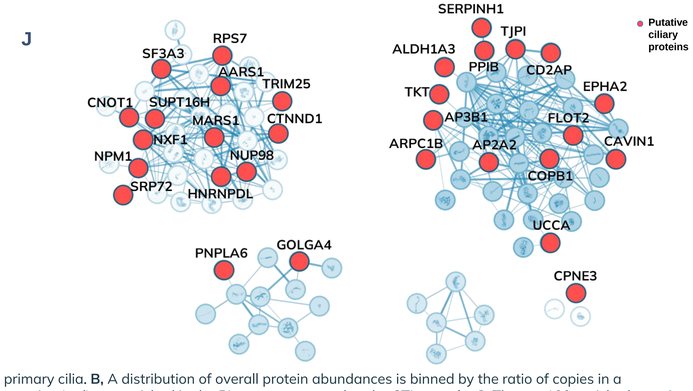

Fig. 4 | A, Confocal micrographs of unphotolabeled (UL) and photolabeled (PL) at user defined primary cilia. **B,** A distribution of overall protein abundances is binned by the ratio of copies in a photolabeled (PL) sample to those in a control (CTL) sample annotated as PL/CTL ratio. Ciliary proteins (red) are enriched in the PL group compared to the CTL sample. **C,** The top 100 enriched proteins were subjected to Gene ontology to reveal cilia related biological process. **D,** Well-known ciliary proteins identified by Microscoop™. **E,** 427 ciliary proteins significantly enriched by Microscoop™. **F,** The 427 enriched ciliary proteins were subjected to Reactome to reveal cilia related pathways. **G,** The ranking of the top 50 protein abundances (PL/CTL), where ciliary proteins are indicated in red and non-ciliary proteins are indicated in grey. **H,** The list of the top 30 non-ciliary proteins (putative ciliary proteins) enriched by Microscoop™. **I,** The top 30 putative ciliary proteins (H) were subjected to Gene ontology to reveal cilia related biological process. **J,** Top 100 ranked proteins were subjected to STRING to reveal protein-protein interaction networks, where the 30 putative ciliary proteins (H) are indicated in red.

Summary

- An innovative platform that combines microscopy, deep learning, two-photon illumination, and mechatronics for advanced image-guided photo-biotinylation in hypothesis-free proteomics
- Fast and precise photo-biotinylation of spatially specific proteins from hundreds of thousands of cells enhances the sensitivity of mass spectrometry
- In mapping the ciliary proteome, 427 known ciliary proteins were enriched, and the validation of previously unreported proteins in primary cilia is underway